Electrochemistry Communications 12 (2010) 402–405

Contents lists available at ScienceDirect

Electrochemistry Communications

journal homepage: www.elsevier.com/locate/elecom

Direct electrochemistry and electrocatalysis of hemoglobin based on poly(diallyldimethylammonium chloride) functionalized graphene sheets/room temperature ionic liquid composite film

Kunping Liu [a,b], Jingjing Zhang [b], Guohai Yang [b], Chunming Wang [a,*], Jun-Jie Zhu [b,*]

[a] School of Chemistry and Chemical Engineering, Lanzhou University, Lanzhou 730000, PR China
[b] Key Lab of Analytical Chemistry for Life Science (MOE), School of Chemistry and Chemical Engineering, Nanjing University, Nanjing 210093, PR China

ARTICLE INFO

Article history:
Received 12 November 2009
Received in revised form 22 December 2009
Accepted 5 January 2010
Available online 11 January 2010

Keywords:
Graphene
PDDA
Room temperature ionic liquid
Biosensors

ABSTRACT

The functionalized graphene nanosheets (PDDA-G) with poly(diallyldimethylammonium chloride) (PDDA) were synthesized and used to combine with room temperature ionic liquid (RTIL). The resulting RTIL/PDDA-G composite displayed an enhanced capability for the immobilization of hemoglobin to realize its direct electrochemistry. Moreover, the RTIL/PDDA-G based biosensor exhibited excellent electrocatalytic activity for the detection of nitrate with a wide linear range from 0.2 to 32.6 μM and a low detection limit of 0.04 μM at 3σ. This work opens a new way to functionalized graphene nanosheets with good biocompatibility and solubility in biosensors.

1. Introduction

Graphene, a monolayer of sp^2 hybridized carbon atoms, had attracted enormous attention since it was first reported in 2004 [1]. The elusive two-dimensional structure of graphene has numerous intriguing properties such as high conductivity, superior mechanical and electronic properties, producing promising potential applications in sensors and electrocatalysis [2,3]. However, graphene is hydrophobic and tends to form agglomerates or even re-graphitized to graphite due to the van der Waals interactions and strong π–π stacking which may limit its further biological applications [4]. Particularly in electrochemical biosensors, the prevention of aggregation is of vital importance for graphene because most of its unique properties are only associated with individual sheets. Thus, great efforts have been made to increase the graphene solubility through covalent or noncovalent functionalization, of which noncovalent strategies, particularly using polyelectrolytes as functional agent, were more favorable than the covalent ones [5,6]. Poly(diallyldimethylammonium chloride) (PDDA), a linear positively charged polyelectrolyte, has been found to be attractive for functionalizing nanomaterials and thus might be used to noncovalently functionalize graphene sheets [7]. Moreover, PDDA has excellent binding capability with graphene and could maintain the electronic structure of graphene. Accordingly, functionalizing graphene with PDDA could be an effective method to increase the solubility, for the extending application in biosensing.

On the other hand, room temperature ionic liquid (RTIL) has long been of intense interest in electrochemical biosensors due to its high ionic conductivity and well biocompatibility for enhanced electrochemical response [8]. More recently, it was found that RTIL could improve the dispersion of graphene, producing RTIL-modified graphene with promising ability to realize the direct electron transfer of glucose oxidase [9]. However, it is still a challenge for the combinations of RTIL with the graphene sheets to fabricate novel biosensors.

Here we present, for the first time, the preparation and characterization of PDDA-functionalized graphene sheets (PDDA-G) by a simple synthetic method, in which PDDA could bind with negatively charged graphene to prevent the aggregation of graphene sheets through electrostatic repulsion. Subsequently, PDDA-G was used to combine with RTIL, resulting in a novel nanocomposite with excellent conductivity, biocompatibility and solubility. In addition, the nanocomposite film was in favor of enhancing protein loading and retaining the bioactivity. Using hemoglobin (Hb) as a model protein, the constructed biosensor displayed a fast electron transfer of Hb and a good electrochemistry activity for the detection of nitrate with wide linear range and low detection limit. Therefore, the present work offers a new avenue to broaden the applications of graphene in electrochemical biosensors.

* Corresponding authors. Tel./fax: +86 25 83594976.
E-mail addresses: wangcm@lzu.edu.cn (C. Wang), jjzhu@nju.edu.cn (J.-J. Zhu).

1388-2481/$ - see front matter © 2010 Elsevier B.V. All rights reserved.
doi:10.1016/j.elecom.2010.01.004

2. Experimental

2.1. Materials and apparatus

Graphite powder (KS-10), Hb and PDDA (MW = 200 000–350 000) were from Sigma. [bmim] [BF_4] was purchased from Lanzhou Institute of Chemical Physics (Lanzhou, China). Hydrazine hydrate was from Nanjing Reagent Co. (Nanjing, China). Electrochemical measurements were performed on a CHI 660a workstation (Shanghai Chenhua, China) with a conventional three-electrode system comprised of a platinum wire auxiliary, a saturated calomel reference and the modified glass carbon (GCE) working electrode. Characteristics were performed via field-emission scanning electron microscopy (FESEM, HITACHI S4800), high resolution transmission electron microscopy (HRTEM, JEOL 2010), Fourier-transform infrared (FT-IR Bruker Vector 22), atomic force microscope (AFM, Agilent 5500) and X-ray powder diffraction (XRD, Shimadzu XD-3A).

2.2. Synthesis of PDDA-functionalized graphene

Graphite oxide (GO) was prepared from graphite powder by a modified Hummers method [10] and then dispersed in water to yield a yellow–brown dispersion by ultrasonication for 2 h, followed by centrifugation to remove any unexfoliated GO. Subsequently, the homogeneous GO dispersion (100 mL) was mixed with 0.5 mL PDDA solution and stirred for 30 min. The resulting mixture was further treated with 0.5 ml hydrazine hydrate and allowed to react for 24 h at 90 °C. Finally, the black PDDA-functionalized graphene (PDDA-G) was collected by filtration and further washed with water.

2.3. Construction of Hb/RTIL/PDDA-G/GCE biosensor

The GCE was first polished with 0.3 and 0.05 μm alumina slurry, and sonicated in ethanol and water successively. For the preparation of Hb/RTIL/PDDA-G/GCE, 10 mL of 0.1 mg ml^{-1} PDDA-G was first mixed with 34 μL of RTIL and sonicated for 1 h to form a homogenous mixture. Then, 5 μL of the mixture was dropped on the pretreated GCE and dried in a desiccator. Finally, the electrode was immersed in 5 mg ml^{-1} hemoglobin solution at 4 °C for 8 h. Hb/RTIL/graphite electrode was also fabricated for comparison using similar process just using graphite instead of PDDA-G.

3. Results and discussion

3.1. Characterization of PDDA-G

The PDDA-G was first characterized by TEM and HRTEM (Fig. 1A). The TEM image of PDDA-G showed a general view of graphene nanoplatelets and the HRTEM image of PDDA-G (inset of Fig. 1A) showed the edge of a graphene nanosheet which clearly illustrated the flake-like shapes of graphene. The XRD pattern (Fig. 1B) showed that the GO (curve b) had a peak centered at 10.0°, while the characteristic peak at 26.4° of graphite (curve a) was absent. After the reduction with hydrazine, no obvious peak was observed in PDDA-G (curve c), indicating the completely reduction of GO. The image of water dispersion of graphene without (left) and with (right) PDDA was displayed in the inset of Fig. 1B. Owing to the noncovalent adsorption of PDDA, the PDDA-G bore a positive charge to avoid aggregation, thus its dispersity in water was greatly enhanced. In contrast, graphene without PDDA functionalization aggregated more readily.

Furthermore, FT–IR spectroscopy was employed to investigate the functionalized and assembly process. As shown in Fig. 1C, PDDA-G (curve a) showed an obvious skeletal vibration adsorption band of the graphene at 1575 cm^{-1} [11]. The absence of the peaks at 1730 cm^{-1} (C=O), 1365 cm^{-1} (C–OH), 1250 cm^{-1} (C–O–C) and 1060 cm^{-1} (C–O) indicated the remove of oxo-groups on GO after reduction [12]. The absorption bands at 2923 cm^{-1} (CH_n), 1633 cm^{-1} (C=C) and 1460 cm^{-1} (C=C) corresponded to the characteristic bands of PDDA, indicating the functionalization of graphene with PDDA [13]. Moreover, RTIL/PDDA-G and Hb/RTIL/PDDA-G (curves c and e) showed a strong adsorption band at about 1065 cm^{-1} which was consistent with the pure RTIL (curve b). This adsorption band could attributed to the B–F stretching vibrations of $[BF_4]^-$ anions [14]. By comparison, the amide I (1645 cm^{-1}) and amide II (1537 cm^{-1}) of Hb immobilized on RTIL/PDDA-G were nearly the same as those of the native Hb (curve d). The slight shift of amide I band from 1658 to 1645 cm^{-1} revealed the interaction between Hb and the RTIL/PDDA-G composite. Therefore, Hb entrapped in the RTIL/PDDA-G composite film retained the essential features of native secondary structure.

In order to confirm the single-sheet nature of the graphene, AFM image of PDDA-G was obtained in tapping mode as shown in Fig. 1D, which revealed the presence of nanoplatelets with uniform thickness. Cross-section analysis of AFM image (Fig. 1E) and the thickness histogram compiled from multiple AFM images (Fig. 1F) revealed the thickness of PDDA-G nanoplatelets was about 1.3 nm, greater than the well exfoliated GO sheets with a thickness of about 0.9 nm. This maybe was due to the presence of the PDDA covered onto both sheet sides.

3.2. Direct electrochemistry of Hb/RTIL/PDDA-G/GC electrode

The direct electrochemistry of Hb modified electrodes was studied by cyclic voltammetry. As shown in Fig. 2A, no current peak was observed at the RTIL/PDDA-G (b) and the PDDA-G (a) modified electrodes, indicating the electro-inactiveness of PDDA-G and RTIL/PDDA-G composite. After combining with Hb, a pair of ill-defined and irreversible redox peaks was observed at the Hb/PDDA-G/GC electrode (curve c) at −0.435 V and −0.202 V, indicating a slow electron-transfer process of Hb. However, when RTIL was introduced into the PDDA-G film, the Hb/RTIL/PDDA-G/GCE showed a stable, well-defined and quasi-reversible redox peaks at −0.360 V and −0.292 V (curve d), with a peak-to-peak separation of about 68 mV, revealing a fast electron transfer. Besides, the current responses were remarkable increased and the redox peaks almost unchanged after continuous potential cycling. These results demonstrated that the composite provided a biocompatible microenvironment for enzyme loading and retaining native bioactivity, while the RTIL played an important role in establishing a fast electron transfer path to facilitate the direct electron transfer of Hb.

The effect of scan rate was shown in Fig. 2B. With an increasing scan rate, the redox peak currents increased simultaneously, accompanied enlarged the peak separation. Moreover, both the cathodic and anodic peak currents increased linearly with the scan rate from 20 to 600 mV s^{-1} (inset of Fig. 2B), indicating a surface-controlled quasi-reversible process. According to Faraday's law, the surface concentration of electroactive Hb (Γ^*) at Hb/RTIL/PDDA-G/GCE was estimated to be 4.25×10^{-10} mol cm^{-2}, which was much larger than the theoretical monolayer coverage of the Hb (1.89×10^{-11} mol cm^{-2}). This indicated that a multilayer of Hb participated in the electron-transfer process in the RTIL/PDDA-G composite film.

3.3. Electrocatalysis of Hb/RTIL/PDDA-G/GCE to reduction of nitrite

In order to study the electrocatalytic activity of Hb immobilized in RTIL/PDDA-G film, its response to the reduction of nitric oxide was explored. Fig. 3A showed the CVs of Hb/RTIL/PDDA-G/GCE in

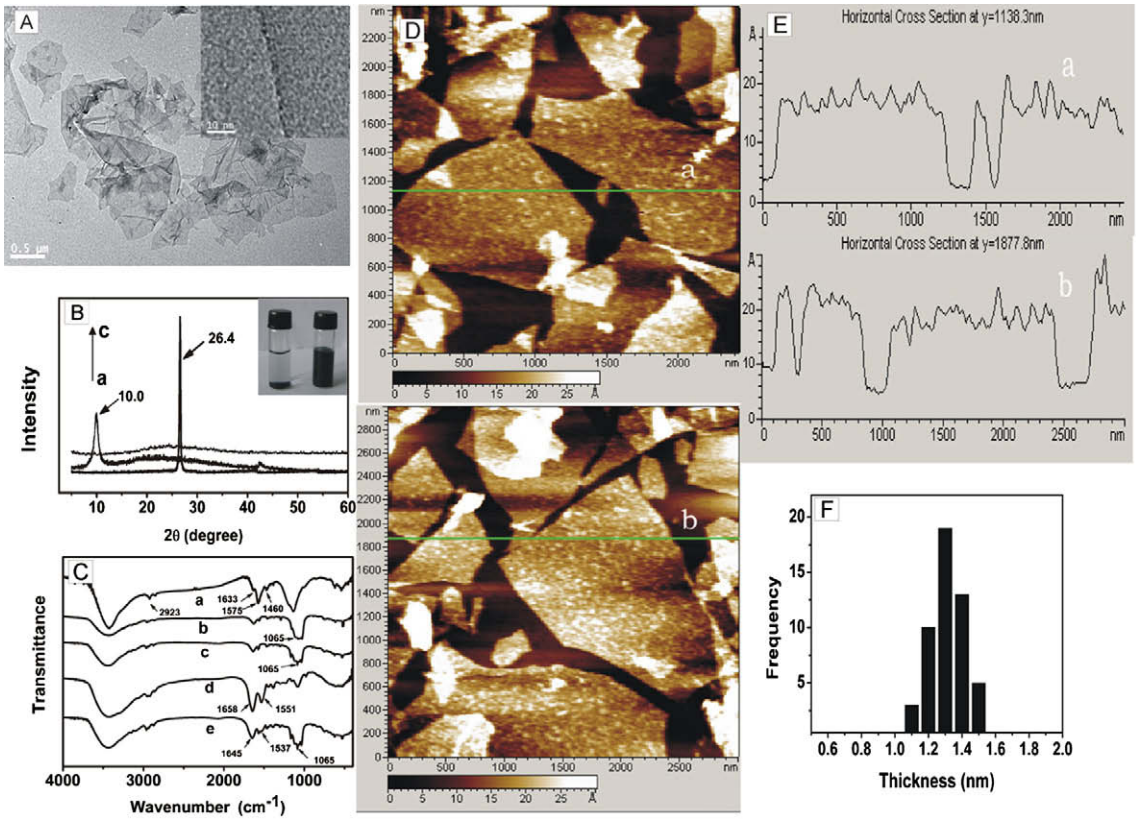

Fig. 1. (A) TEM and HRTEM (inset) image of PDDA-G. (B) XRD patterns of (a) graphite, (b) GO, and (c) PDDA-G. Inset: photo of aqueous dispersion (1 mg mL^{-1}) of graphene prepared without PDDA (left) and with PDDA (right). (C) FT–IR spectra of (a) PDDA-G, (b) RTIL, (c) RTIL/PDDA-G, (d) Hb, and (e) Hb/RTIL/PDDA-G. (D) AFM image of PDDA-G. (E) Cross-section analysis along the lines shown in AFM image. (F) Histogram showing the distribution of sheet heights measured on 50 different sheets from multiple AFM images.

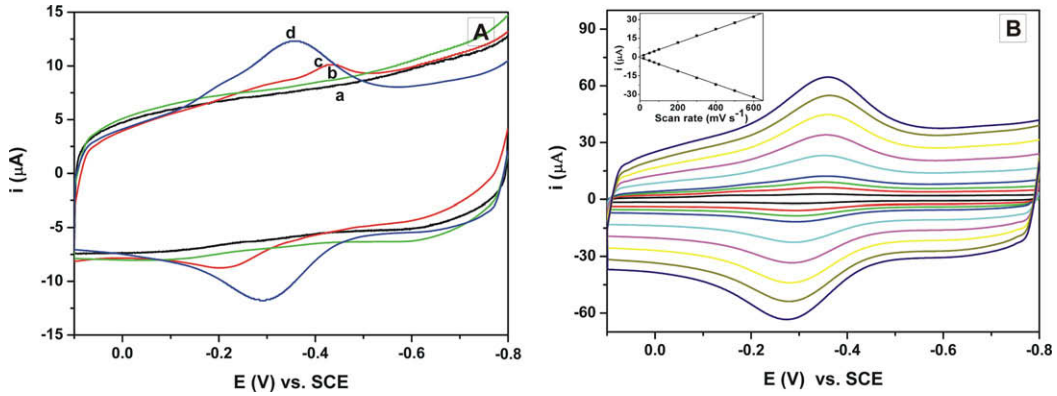

Fig. 2. (A) CVs of (a) RTIL/PDDA-G, (b) PDDA-G, (c) Hb/PDDA-G, and (d) Hb/RTIL/PDDA-G modified GCE in 0.1 M pH 7.0 PBS at 0.1 V s^{-1}. (B) CVs of Hb/RTIL/PDDA-G modified GCE at scan rate of 20, 50, 75, 100, 200, 300, 400, 500, and 600 mV s^{-1} (from inner to outer curve) in 0.10 M pH 7.0 PBS. Inset: plots of peak currents vs. scan rates.

NaAc–HAc buffer containing different concentrations of $NaNO_2$. In the absence of $NaNO_2$, only the redox peaks of Hb were observed at −0.152 V and −0.213 V. However, with the addition of $NaNO_2$, a well-defined cathodic peak for the reduction of NO which came from the disproportionation reaction of nitrite in acidic solution could be observed at about −0.580 V and the peak current increased with the increase of $NaNO_2$ concentration [15]. In contrast, no significant reduction peak of NO was observed on the PDDA-G and RTIL/PDDA-G modified GCE (inset of Fig. 3A). This phenomenon revealed that the immobilized Hb retained high electrocatalytic activity to nitrite which could be attributed to the excellent conductivity and biocompatibility of RTIL/PDDA-G composite film.

Fig. 3B illustrated the steady-state response of the Hb/RTIL/graphite (curve a) and Hb/RTIL/PDDA-G (curve b) with successive additions of $NaNO_2$ into NaAc–HAc buffer solution at an applied potential of −0.580 V. Hb/RTIL/graphite showed a very small response toward the addition of $NaNO_2$ and could be completely negligible when compared to the Hb/RTIL/PDDA-G. The calibration curve of Hb/RTIL/PDDA-G in the inset of Fig. 3B showed a good linear relationship with the concentration of nitrite from 0.2 to 32.6 μM with a correlation coefficient of 0.998 (n = 16). The detection limit was estimated to be 0.04 μM at 3σ, which was obviously lower than previous report [16]. This lower detection limit can be attributed to the combination of PDDA-G and RTIL, which not only

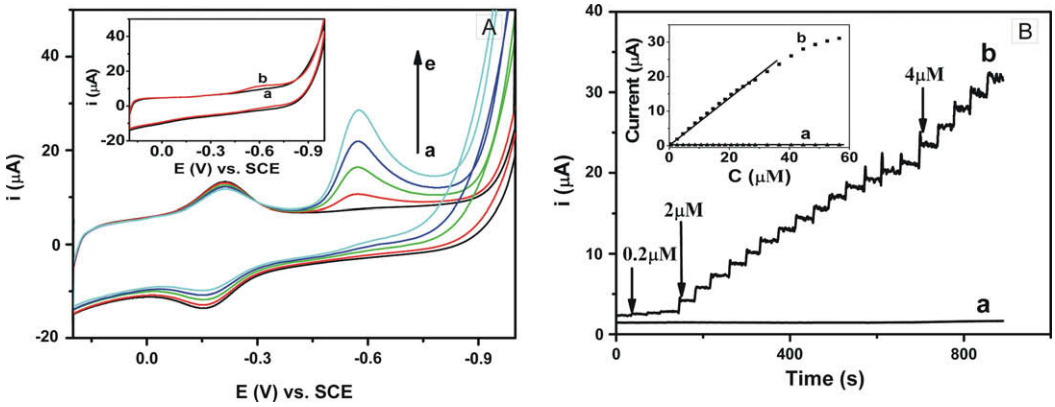

Fig. 3. (A) CVs of Hb/RTIL/PDDA-G modified GCE in 0.20 M pH 2.0 NaAc–HAc buffer containing: (a) 0, (b) 2, (c) 6, (d) 10, and (e) 16 μM of $NaNO_2$. Inset: CVs of (a) PDDA-G/GCE and (b) RTIL/PDDA-G/GCE in 0.20 M pH 2.0 NaAc–HAc buffer containing 16 μM of $NaNO_2$. (B) Typical amperometric current–time response curves of the Hb/RTIL/graphite (a) and Hb/RTIL/PDDA-G (b) biosensor upon successive addition of $NaNO_2$ into 0.20 M pH 2.0 NaAc–HAc buffer solution. Applied potential: −0.58 V. Inset: linear relation between the amperometric response and NO_2^- concentration.

offered a biocompatible surface for Hb loading, but also provided a sensitive electric interface for further biosensing.

4. Conclusion

In this work, PDDA-functionalized graphene nanosheets with good conductivity, solubility and biocompatibility were successfully synthesized and applied in Hb immobilization and biosensor construction. By combining the advantages of PDDA-G and RTIL, the proposed biosensor showed a fast direct electron transfer of Hb. Moreover, it also displayed excellent analytical performance in the determination of nitrite with wide linear range and low detection limit. The present strategy definitely paves a way for the functionalization of graphene sheets with good biocompatibility and solubility, thus provides a novel and promising platform for the study of the biological application of graphene.

Acknowledgements

The authors acknowledge the National Natural Science Foundation of China (Nos. 20635020 and 20775030) for financial support of this work. This work is also supported by 973 Program (No: 2006CB933201).

References

[1] K.S. Novoselov, A.K. Geim, S.V. Morozov, D. Jiang, Y. Zhang, S.V. Dubonos, I.V. Grigorieva, A.A. Firsov, Science 306 (2004) 666.
[2] F. Schedin, A.K. Geim, S.V. Morozov, E.W. Hill, P. Blake, M.I. Katsnelson, K.S. Novoselov, Nat. Mater. 6 (2007) 652.
[3] L.H. Tang, Y. Wang, Y.M. Li, H.B. Feng, J. Lu, J.H. Li, Adv. Func. Mater. 19 (2009) 2782.
[4] S. Niyogi, E. Bekyarova, M.E. Itkis, J.L. McWilliams, M.A. Hamon, R.C. Haddon, J. Am. Chem. Soc. 24 (2006) 7720.
[5] S. Stankovich, R.D. Piner, X.Q. Chen, N.Q. Wu, S.T. Nguyen, R.S. Ruoff, J. Mater. Chem. 16 (2006) 155.
[6] H. Liu, J. Gao, M.Q. Xue, N. Zhu, M.N. Zhang, T.B. Cao, Langmuir 25 (2009) 12006.
[7] Z.A. Xu, N. Gao, S.J. Dong, Talanta 68 (2006) 753.
[8] G.C. Zhao, M.Q. Xu, J. Ma, X.W. Wei, Electrochem. Commun. 9 (2007) 920.
[9] C.S. Shan, H.F. Yang, J.F. Song, D.X. Han, A. Ivaska, L. Niu, Anal. Chem. 81 (2009) 2378.
[10] W.S. Hummers, R.E. Offeman, J. Am. Chem. Soc. 6 (1958) 1339.
[11] C. Nethravathi, M. Rajamathi, Carbon 46 (2008) 1994.
[12] Y.C. Si, E.T. Samulski, Nano Lett. 8 (2008) 1679.
[13] D.Q. Yang, J.F. Rochette, E. Sacher, J. Phys. Chem. B 109 (2005) 4481.
[14] R. Holomb, A. Martinelli, I. Albinsson, J. Raman Spectrosc. 39 (1986) 793.
[15] M.H. Barley, K.J. Takcuchi, T.J. Meyer, J. Am. Chem. Soc. 108 (1986) 5876.
[16] J.T. Pang, C.H. Fan, X.J. Liu, T. Chen, G.X. Li, Biosens. Bioelectron. 19 (2003) 441.